DOI: 10.2478/sspjce-2025-0007

Evaluating Compressive Strength in 3D-printed Concrete Structures: A Comparative Study of ANSYS Simulations and Experimental Data

Salhah Mohammed[1*], Hana Aljewifi [1], Hafeth Bu Jldain[1]

[1]University of Omar Al-Mukhtar, Elbeida, Libya
Faculty of Engineering
[*]e-mail: lalyabdo1033@gmail.com

Abstract

This paper investigates the use of 3D printing technology in concrete construction, with a focus on the compressive strength of 3D-printed structures. The study highlights the growing interest in 3D-printed concrete (3DPC) due to its potential for creating complex geometries, optimizing material usage, and reducing environmental impact.

The research also examined various experimental studies that tested 3D-printed concrete samples, focusing on the differences in material composition and additives that affect compressive strength. The results of the simulations using ANSYS program were compared with experimental data, revealing discrepancies due to factors such as anisotropy, curing methods, and challenges in accurately modeling material behavior in simulations. While the simulation results closely aligned with experimental findings in some cases, significant variations were observed in others, highlighting the need for improved modeling techniques.

Despite these challenges, the study underscores the potential of 3D printing in revolutionizing the construction industry. The findings suggest that continued advancements in both material science and simulation tools are necessary to fully realize the benefits of 3D-printed concrete in large-scale structural applications.

Keywords: 3D printed concrete, ANSYS modeling, mechanical behavior, material properties

1 Introduction

3D concrete printing (3DCP) is a rapidly developing technology that integrates digital innovations with advancements in material science to enable free-form construction without the need for formwork. As an additive manufacturing method, structures are created through the sequential deposition of material in layers [1]. Consequently, the use of additive manufacturing in concrete has become a major focus for both academic and industrial research worldwide, leading to a substantial increase in 3DCP projects since 2015.

The principle of additive manufacturing lies in the consecutive stacking of two-dimensional layers of material to form a three-dimensional object. A universally accepted definition of 3D printing remains elusive, as a wide range of definitions and terminologies are employed or combined to describe this concept. Broadly, it can be defined as "the fabrication of objects through the controlled deposition of material using a print head, nozzle, or other printing technologies, in contrast to traditional manufacturing processes based on material removal" [2]; see Figure 1.

Figure 1: 3D printing of construction

3D printing technology has gained extensive attention because it offers faster construction, lower costs, reduced labor requirements, and fewer errors compared with traditional approaches [3]. Continuous improvements in printing materials and equipment are considered strategic goals by many companies worldwide. At the academic and industry level, research interest in applying 3D printing to construction has grown exponentially over the past decade. Considering global demand to reduce CO2 emissions, innovative construction technologies are required not only to support sustainable practices but also to lower project and facility management costs while enhancing competitiveness. Formwork, which typically accounts for about 40% of total concrete construction costs, can be eliminated when applying 3DCP, thus reducing both project duration and expenses [4].

Three-dimensional concrete printing provides transformative opportunities for the construction sector. Among its primary advantages is exceptional design flexibility, enabling the realization of complex and customized structures that cannot easily be achieved with conventional methods. Furthermore, 3DCP allows for the integration of multiple materials, improving both functional and aesthetic performance while enabling rapid, cost-effective construction in areas affected by disasters or economic constraints. The precision of the process minimizes waste, reduces errors, and contributes to more sustainable and economical building practices. Overall, 3DCP has the potential to redefine design, safety, efficiency, and sustainability in the future construction landscape [5–8]. Despite its benefits, the implementation of 3DCP presents several notable challenges. A significant concern is the potential reduction in conventional construction jobs, as automation limits the need for manual tasks such as traditional concrete casting. Another challenge is scalability, since existing printers are often restricted in size, making them unsuitable for very large projects without further technological development. Additionally, the technology requires new skill sets, which demand specialized training in advanced manufacturing methods. Equally important, the absence of standardized design codes and regulations hinders widespread adoption, as construction enterprises encounter difficulties

complying with current building standards. Addressing these challenges is crucial for the successful integration of 3DCP into mainstream construction [7, 9].
Previous research indicates that many experimental formulations have been tested in search of optimal mix designs. Most mixtures incorporated a large proportion of fine particles, with limited studies addressing the use of coarse aggregates in 3DCP. While admixtures such as superplasticizers, accelerators, and retarders were incorporated in mixes to regulate open time and setting time [10].

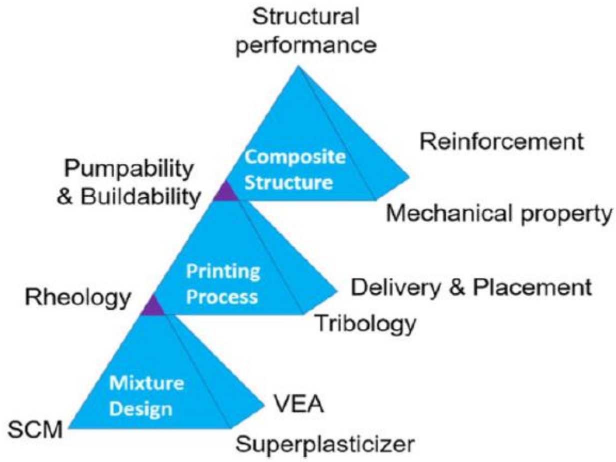

Figure 2: Multilevel design for 3DP material [10]

In recent research, conducting extensive experimental campaigns to optimize mix designs is often economically prohibitive. Consequently, the investigation of numerical approaches for the purpose of analyzing the behavior of additively manufactured structures acquires critical significance [11]. Nevertheless, in the fabrication of large structures or under complex variables, purely experimental methods become impractical, highlighting the importance of computational strategies.
Both numerical and analytical methods have therefore attracted considerable interest as alternatives to time-consuming experimental procedures. The study conducted by Feng et al. [12] investigated the mechanical properties of cementitious structures fabricated through 3D printing, particularly their compressive strength, elastic modulus, and failure mechanisms. Due to their layered microstructure, the study focuses on these materials' anisotropic behavior and proposes a comprehensive stress-strain relationship and a failure criterion. It specifically analyzed the compressive strength of 3D printed cement-based models produced using a Spectrum Z510 3D printer, with a mixture of mortar powder (ZP150) and binder (ZB60) with a binder volume fraction of 21.8%. The X-direction had the highest compressive strength (16.8 MPa for 50 mm cubes), the Y-direction had an intermediate strength (11.6 MPa), and the Z-direction had the lowest strength (13.2 MPa) due to weaker inter-layer bonds. These findings suggest that the compressive properties change substantially during the stacking process. This confirms the orthotropic behavior of these materials, whose mechanical properties are clearly affected by the printing process. Additionally, the study noted that binder content and printing speed play an important role in the quality of inter-layer bonding. Faster printing in the X-direction produces stronger inter-filament bonding, which improves compressive strength, while longer curing times contribute to higher compressive strength.

Based on the exploratory results, this study proposed a quadratic function model of the stress-strain relationship of 3D printed cement-based materials under compression, which was closely integrated with the data. These findings reinforce the importance of the printing process and fabric composition in determining the mechanical properties of 3D printed structures. The developed stress-strain relationship and failure model serve as a foundational framework for planning and analyzing 3D printed cementitious structures. Shakor et al. [13] conducted a comprehensive investigation on 3D printed cement mortar specimens using inkjet printing technology, focusing on their mechanical properties, particularly compressive strength. The primary objective of the study was to determine the optimal compressive strength of 3D printed structural members across three planes (XY, XZ, and YZ) and to analyze their mechanical behavior under compression. The authors emphasized that research involving the experimental and numerical analysis of printed cement mortar is relatively scarce, highlighting a gap in the literature. The materials used in this study comprised a blend of calcium aluminate cement (CAC), ordinary Portland cement (OPC), and fine sand.
Various tests were conducted to assess the compressive strength, modulus of elasticity, and Poisson's ratio of the printed specimens. The compressive strength was evaluated using cubes of size 50 mm x 50 mm x 50 mm, and results were obtained under controlled conditions. The study revealed that the compressive strength varied significantly depending on the loading direction. Notably, the strength was highest in the XY plane (approximately 24 MPa) and lowest in the YZ plane (approximately 10 MPa), demonstrating the orthotropic properties of the printed mortar. The findings indicated that the layered structure created a bond between the layers, which resulted in anisotropic mechanical properties. The authors also reported that failure mechanisms were predominantly along the layer interfaces, leading to delamination and cracking when subjected to loading, particularly in the direction parallel to the layers. Furthermore, the study explored the impact of materials on compressive strength, noting that the composition and properties of the cement mortar directly influenced mechanical performance. The authors concluded that optimizing the material properties, including the ratios of CAC and OPC, is essential for enhancing the performance of 3D printed structures. Delavar et al. [14] conducted a study, the objective of their research was to examine the compressive strength and failure mechanisms of 3DPC walls subjected to in-plane seismic loading. They aimed to develop strength design equations that would incorporate both diagonal shear failure and flexural failure mechanisms. This study is significant as it addresses the gap in code-based design guidelines for 3DPC structures, which is crucial for their acceptance in the construction industry.
In their methodology, Delavar et al. (2022) investigated the compressive strength of 3DPC walls that were reinforced with bed-joint reinforcement (ladder mesh) and internal reinforced concrete (RC) elements. They derived strength prediction equations based on principles from masonry wall design, specifically referencing TMS 402/602-16. The authors validated their proposed equations through numerical modeling using OpenSees, analyzing four different configurations of 3DPC walls categorized as either shear-critical or flexure-critical based on their infill patterns and reinforcement layouts. The key findings from their study revealed several important insights. Firstly, the proposed equations for predicting the in-plane strength of 3DPC walls considered the contributions of both printed concrete and reinforcement elements. The numerical validation showed a strong correlation between predicted and simulated failure mechanisms, with a maximum discrepancy of approximately 20% observed in flexure-critical walls. Furthermore, shear-critical walls primarily exhibited diagonal shear

failure, predominantly influenced by their infill patterns, while flexure-critical walls failed due to bending, emphasizing the role of reinforcement in enhancing compressive performance.
The study also highlighted the influence of reinforcement on compressive strength. The inclusion of bed-joint reinforcement significantly increased the shear resistance of the walls, which indirectly contributed to higher compressive strength. Additionally, the presence of grouted cells and RC columns was crucial for resisting lateral forces, thereby enhancing the overall load-bearing capacity of the walls.
Li, Hu, and Shahzad [15] investigated the anisotropic behavior of 3DPC utilizing finite element simulation, focusing on its mechanical properties and the effects of material composition and printing parameters. This research aimed to address the challenges associated with the anisotropic nature of 3DPC, which results from the layer-by-layer deposition process, leading to defects such as voids and weak interfacial bonds. These defects significantly affect the material's mechanical performance, especially its compressive strength, making it crucial to understand and mitigate these issues for reliable construction applications.
The authors conducted compression tests on 3D printed concrete 3D shapes measuring 100 mm x 100 mm x 100 mm. They utilized concrete blends of changing qualities (C20, C35, C50), the labels C20, C35, and C50 are used as simplified designations to denote the approximate target compressive strength level (in MPa) of the different concrete mixes, rather than referring to formal standardized classes like C16/20 or C20/25. And included materials like basalt and glass fibers to assess their impact on compressive strength. The performance of 3D printed concrete was compared to that of conventional cast concrete to evaluate anisotropic behavior. The results showed that the compressive strength of 3DPC varied significantly with direction, generally being lower than that of cast concrete, with the X-direction exhibiting higher strength than the Y and Z directions. The study also examined the effects of fiber additives, finding that the inclusion of fibers improved compressive strength, particularly in the X-direction. The findings concluded that the anisotropic behavior of 3DPC is significantly influenced by the printing process and material composition. This emphasizes the need for improved simulation techniques to accurately reflect the mechanical properties of 3DPC, considering the variability introduced by different materials and printing parameters. The results provide important insights for the design and application of 3D printed concrete, paving the way for future advancements in this innovative engineering material.
The anisotropic behavior of 3D printed concrete is evident in its hardened state as a result of variations at the interfacial regions between successive layers. While the interfacial bond properties and overall mechanical characteristics of 3D printed concrete have been investigated individually in several studies, the reported patterns of anisotropic behavior vary significantly across the literature. Moreover, the direct influence of interfacial bond properties on the anisotropic mechanical response of 3D printed concrete remains insufficiently addressed in current research. A deeper understanding of the interplay between interfacial bonding, mechanical performance, and variations in anisotropic behavior is essential for the future structural design and optimization of 3D printed systems [16]. In this research, the application of ANSYS software plays a central role in modeling and simulating the behavior of 3D printed concrete. Numerical modeling provides a means to evaluate the reliability of structural responses beyond the limitations imposed by instability inherent in physical experiments. By conducting simulations under controlled and repeated loading conditions, ANSYS enables comprehensive verification of experimental results, thereby ensuring greater accuracy and robustness in the analysis. A set of comparative tests has been conducted under identical loading

scenarios, followed by full-scale simulations and analyses. This approach allows the differentiation of results across specimens and highlights the impact of variations in the printed concrete mix on compressive strength. Such comparisons offer valuable insights into how different mixtures influence anisotropic mechanical performance, shedding light on the broader implications for design and construction using 3D printing technology.
The purpose of this study is to conduct a comparative assessment between experimental findings and numerical modeling performed using ANSYS 2024. The investigation specifically addresses the anisotropic properties of 3D printed concrete and emphasizes the analysis of its compressive strength. Through this comparison, the study aims to evaluate the correlation between experimental test results and numerical simulations.

2 Methodology

2.1 Theories specimen loading

Given the inherent anisotropic characteristics of three-dimensional printed materials, it is essential to evaluate their compressive strength across multiple orientations. Typically, researchers investigate three primary loading directions: Orientation-I (O-I, perpendicular to the layers), Orientation-II (O-II, lateral), and Orientation-III (O-III, longitudinal), as illustrated in Figure 3. A variety of specimen geometries, including saw-cut cubes, cylinders, and prisms, have been utilized in compressive tests by various researchers. To ensure accurate results, the surface of the test specimen must be either level or appropriately capped [17].

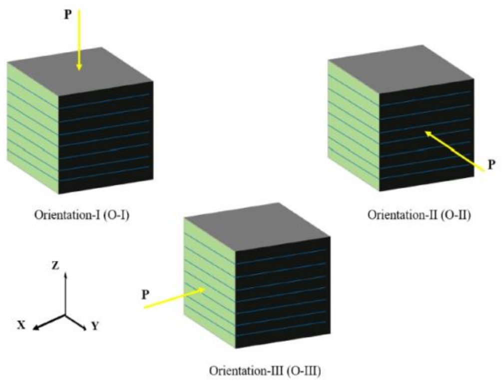

Figure 3: Loading directions for compression testing of 3D printed objects

2.2 Determine the samples: sizes, findings of previous researches

Several relevant studies were selected for comparison, each conducted under distinct conditions with variations in mix design. Diverse materials were incorporated to enhance workability and cohesion after layer deposition. Additives such as fly ash and silica fume were employed as supplementary cementitious materials to improve binding properties. Furthermore, mix proportions were designed to control fluidity, with the water-to-cement ratio (w/c) ranging from 0.28 to 0.6. Table 1 summarizes the experimental results from the reviewed studies.

Table 1: Summary of compressive strength test results from various studies

References	**Test type**	**Testing age** (days)	**Sample size** (mm)	**Test results**
Özalp et al. (2020) [18]	Compressive Strength	28	100 × 100 × 100	White cement mixtures (62.8-64), Grey cement mixture (57.9-59.8) MPa
Benamara. (2022) [19]	Compressive Strength	28	40×40×40	42~52 MPa
Baz et al. (2020) [20]	Compressive Strength after flexural test	3, 7, and 28	40 × 40 × 160	46-62.5 MPa
Panda et al. (2019) [21]	Compressive Strength	4, 7 and 28	50 × 50 × 50	Mix 1, mix 2 and mix 3: 36-57 MPa
Meurer et al. (2021) [22]	Compressive Strength	28	40 × 40 × 40	Slight anisotropy observed, reduction in compressive strength by up to 25%
Panda et al. (2017) [23]	Compressive Strength	28	40 × 40 × 40	19.40-26 MPa
Sanjayan et al. (2018) [24]	Compressive Strength	7	50 × 25 × 30	19-22 MPa
Wern et al. (2024) [25]	Compressive Strength	7 and 28	50 × 50 × 50	Increased strength with curing; S0.40 highest (60.2 MPa)

2.3 Material properties

The material properties implemented in the model were primarily sourced from the referenced experimental study, with key values summarized in Table 2. For parameters not specified therein, values were assumed in accordance with the American Concrete Institute (ACI) code provisions. The loading conditions and the fundamental test methodology for model not specified were defined based on the standard test method ASTM C349-18.

Table 2: Materials properties used in simulation model

Ref.	**Özalp et al. (2020)** [18]					
	Nozzle (mm)	*f'c* (MPa)	γ (kg/m^3)	E	ν	Loading
Value for CEM I 52.5 R (White)	32, 40 and 50	62.8	2350	Not Provided	Not Provided	~0.6 ± 0.2 MPa/s
Value for CEM I 42.5 R (Grey)		57.9				
Ref.	**Benamara. (2022)** [19]					
	40×10	~65	2138	Not Provided	Was assumed as 0.5	2500 KN
Ref.	**Baz et al. (2020)** [20]					
Parallel to layers	40×10	~62.5	Not provided			Standard Testing Method (ASTM C349-18)
Perpendicular to layers		~32.7				
Ref.	**Panda et al. (2019)** [21]					
Parallel to layers	20 × 20	38	Not provided			Standard: BS EN 196-1:2016
Perpendicular to layers		32				
Ref.	**Meurer et al. (2021)** [22]					
Parallel to layers	Round (27) and rectangula r (45)	~63.2	Not provided			-
Perpendicular to layers		~54				
Ref.	**Panda et al. (2017)** [23]					
Parallel to layers	40×10	~52	Not provided			100 kN
Perpendicular to layers		~60				
Ref.	**Sanjayan et al. (2018)** [24]					
	25 × 15	22		Not provided		20 MPa
Ref.	**Wern et al. (2024)** [25]					
	15 × 40	~60.2	2480	Not provided		Test standard: BS EN 196-1:2016

Note: values not specified were assumed as (*f'c*= 28 MPa, E= 200000 MPa, *ν* =0.2).

2.4 The simulation model

The numerical simulation model was established through a series of clearly defined stages in order to replicate the experimental compression tests and to ensure full reproducibility. The modeling procedure can be summarized as follows:

2.4.1 Material properties

The material properties incorporated into the model were primarily obtained from the corresponding experimental studies, as presented in Table 2. For parameters that were not explicitly provided, appropriate values were assumed based on the recommendations of the ACI building code.

2.4.2 Specimen geometry

The geometry of the specimens was generated according to the dimensions specified in Table 1, thereby maintaining consistency with the experimental reference studies.

2.4.3 Element type and meshing

The specimens were discretized using SOLID187 three-dimensional 10-node quadratic elements available in the ANSYS element library for cylinder, cubic, and rectangular specimen. These elements were chosen for their effectiveness in simulating the nonlinear behavior of concrete under compression and their accuracy in capturing irregular stress distributions. The mesh was constructed with a characteristic element size of 0.2.

2.4.4 Boundary conditions and loading

Boundary conditions were defined to reproduce the constraints of a standard uniaxial compression test. The bottom surface of the specimen was fully restrained in all translational degrees of freedom, while the top surface was left unconstrained except in the vertical direction, where the compressive load was applied. The loading was implemented as a uniformly distributed pressure acting perpendicularly on the top surface, with the loading rate defined consistently with the procedure described in Section 2.3.

2.4.5 Simulation execution

Upon completion of meshing and the assignment of boundary conditions, the model was executed in ANSYS. The resulting stress–strain responses were extracted during post-processing, allowing for a comprehensive evaluation of the compressive strength and facilitating direct comparison with the experimental findings.

3 Simulation result and discussion

3.1 Result and discussion

Figure 4 displays values from the simulation findings for the samples that were in close agreement with the experimental data. The small differences between the simulated and actual test circumstances, together with certain challenges in entering the material properties and elucidating the additives and their effects in the simulation, are the reasons for this small discrepancy.

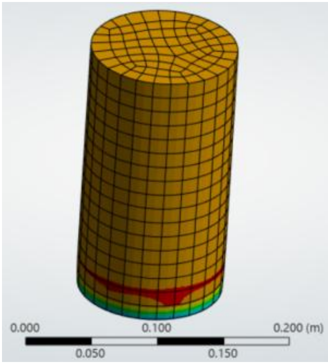

Benamara, (2022) [19]

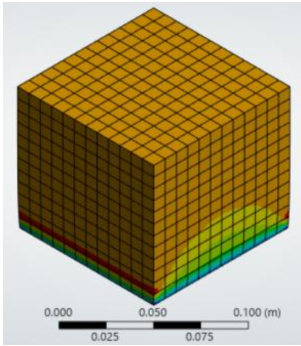

Özalp et al. (2020) [18]

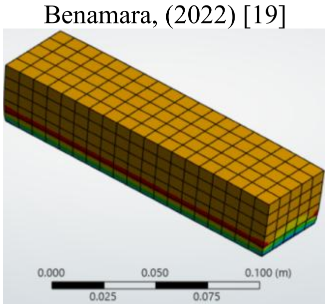

Baz et al. (2020) [20]

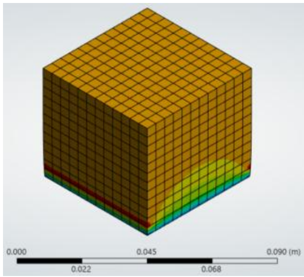

Panda et al. (2019) [21]

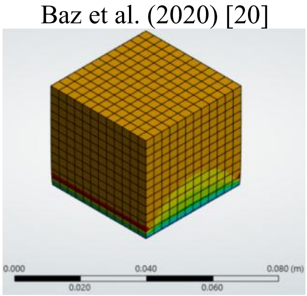

Meurer et al. (2021) [22]

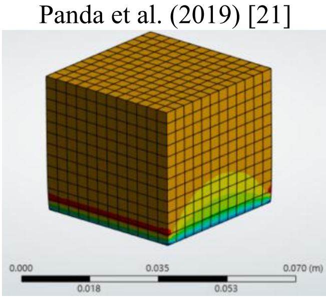

Panda et al. (2017) [23]

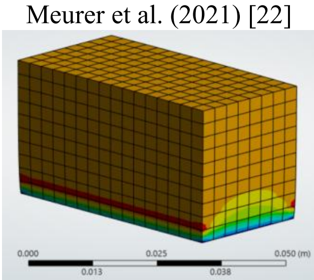

Sanjayan et al. (2018) [24]

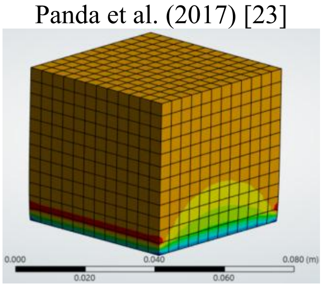

Wern et al. (2024) [25]

Figure 4: Finite element simulation models of compressive strength tests from various studies

A comparison between simulation results and experimental data from various studies reveals significant variations in the accuracy of these simulations, with error percentages highlighting the extent of discrepancies. The following overview examines each study, identifying the causes of disparities, which are primarily attributable to differences in simulation inputs, material properties, and ambient factors.

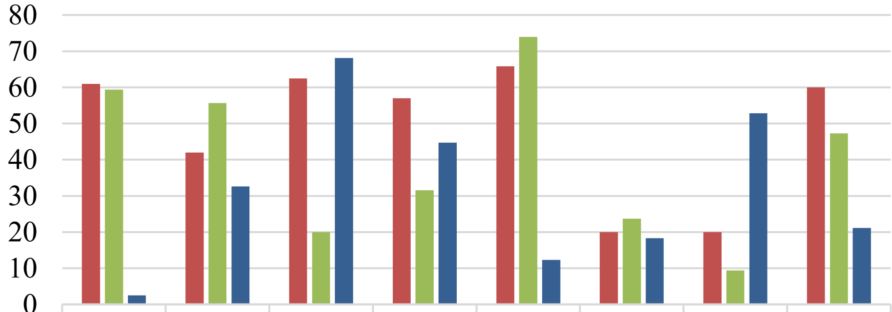

	(a)	(b)	(c)	(d)	(e)	(f)	(g)	(h)
Exp. Result [MPa]	60,95	42	62,5	57	65,8	20	20	60
Minimum [MPa]	59,411	55,701	19,947	31,539	73,919	23,654	9,4289	47,308
Error %	2,53	32,62	68,08	44,67	12,34	18,27	52,86	21,15

Figure 5: Comparison between experimental results and minimum computed values (MPa)

The results from both experiments and simulations in [18] (Fig. 5a) demonstrate close agreement, with a low error percentage of 2.53%. This indicates that the material characteristics and conditions in both the experimental and simulation settings were closely aligned. The minor discrepancy may originate from slight inaccuracies in modeling the material's behavior under stress, which might not fully capture real-world imperfections such as micro-cracks or variations in material composition. In contrast, the simulation results in [19] (Fig. 5b) show a significant overestimation compared to the experimental measurements, with a high error of 32.62%. This substantial discrepancy may be due to challenges in accurately replicating the material characteristics, particularly concerning additives or curing processes. Environmental factors during testing, such as humidity or temperature, which were not fully accounted for in the simulation model, may have contributed to this overestimation.

For [20], the simulated compressive strength recorded a considerable discrepancy with the experimental value, resulting in an error of 68.08%. This indicates a significant problem in accurately representing the material properties in the simulation. The experimental result is more than three times higher than the simulated value, potentially stemming from the model's failure to effectively capture the complex behavior of the materials used. The higher strength of the printed samples may be attributed to additional compaction pressure during the printing process, which expels air pockets and results in a denser matrix. Factors such as specific mix design, additives, and curing conditions likely contributed to this observed discrepancy (Fig. 5c). The simulation for [21] (Fig. 5d) yielded a result with an error of 44.67% lower than the experimental value, indicating a significant underestimation. This variation may originate from oversimplified assumptions in the simulation model, particularly in representing the geopolymer material. The precise control of environmental factors and optimal material

composition achieved in the experiments, which may not have been fully replicated in the simulation, likely contributed to the higher experimental strength.
Conversely, the simulation for [22] (Fig. 5e) overestimated the compressive strength with an error of 12.34%. This suggests that the model overestimated the material's capabilities, potentially due to simplified conditions that neglected real-world imperfections such as slight mix variations or microstructural defects. Additionally, overly optimistic assumptions regarding additive effectiveness or material uniformity could explain the higher simulated strength. The simulation result for [23] is slightly higher than the experimental value, with an error of 18.27%, indicating a reasonably good correlation. This discrepancy may arise from slight inaccuracies in the material model or minor variations in experimental conditions, such as temperature or humidity. The simplification of certain complex factors in the simulation may have led to a modest overestimation of the predicted strength, as illustrated in Fig. 5f.
A notable error of 52.86% is observed between the simulated and experimental results for [24] (Fig. 5g). This discrepancy could originate from limitations in modeling the specific geopolymer formulation. The extrusion pressure during printing likely enhanced compaction and strength in the actual test specimens—a factor influenced by the curing process and the unique characteristics of the binders—which may not have been adequately captured in the simulation, leading to an underestimation of compressive strength. Finally, for the study in [25] (Fig. 5h), the simulation reported a strength with an error of 21.15% lower than the experimental finding. This discrepancy may be attributed to variations in water-to-cement ratios and differing curing periods among the samples, factors that are challenging to precisely evaluate and incorporate into the simulation model. Additionally, difficulties in accurately representing the environmental conditions and the true material properties within the simulation likely contributed to this variability. In summary, the error percentages underscore the challenges in achieving precise alignment between simulation and experimental results, emphasizing the need for refined modeling approaches that better account for material behavior, environmental conditions, and process-related factors.
To strengthen the scholarly contribution of the work, the discussion section has been extensively redeveloped to include a rigorous critical analysis. This enhanced discussion probes the fundamental reasons for the observed computational deviations, connecting them directly to specific shortcomings in existing modeling paradigms for 3DPC. Consequently, the new subsection 3.2, offers a novel and actionable framework, establishing a clear and original contribution to the field. And limitation of this comparative study is a mesh sensitivity analysis was not conducted with deferent element sizes, and also, that it directly compares strengths from different specimen sizes without normalizing for the size effect. Future work should involve applying size effect laws to normalize all compressive strength values to a standard specimen size (e.g., 100 mm cubes) to enable a more rigorous and direct comparison of material performance independent of structural geometry.

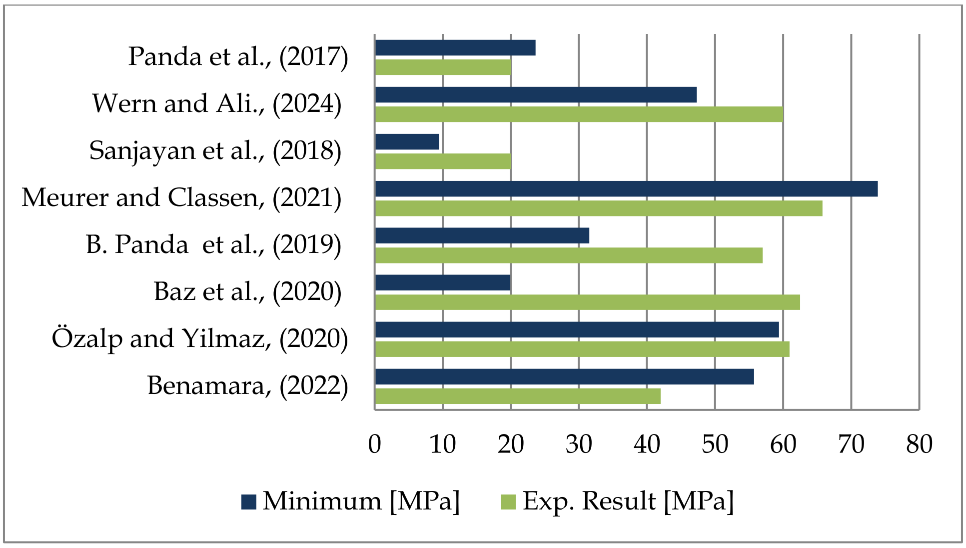

Figure 6: Comparison of experimental and minimum simulated compressive strength results from various studies

3.2 Strategies for enhanced ANSYS modeling

The discrepancies observed between the experimental and simulation results highlight the complexities inherent in modeling 3D printed concrete. To enhance the accuracy and predictive capability of finite element models in ANSYS, the following specific strategies are recommended for future work:

1. Refinement of material models:

- Move beyond linear elastic or simplistic plastic models. The CONCRETE (SOLID65) material model in ANSYS, or more advanced microplane or damage-plasticity models, should be employed to better capture the nonlinear behavior, cracking, and crushing failure of concrete.
- Explicitly model the anisotropic material properties by defining different elastic moduli, Poisson's ratios, and strengths for the X, Y, and Z directions based on experimental data for each printing orientation.

2. Incorporation of imperfections and interfaces:

- Introduce cohesive zone models (CZMs) at the inter-layer interfaces to simulate the potential weak bonds and delamination behavior, which is a critical failure mechanism in 3DPC.

- Model intrinsic voids and porosity within the printed filaments using stochastic methods or by explicitly incorporating simplified void geometries based on micro-CT scan data. This can significantly affect stress concentrations and ultimate strength.

3. Enhanced calibration and validation:

- Calibrate the simulation model not only against ultimate compressive strength but also against the full stress-strain curve and the observed failure mode. A model that matches the strength but not the stiffness or fracture pattern is incomplete.

- Perform a sensitivity analysis to identify the material parameters (e.g., tensile strength, fracture energy) to which the model's output is most sensitive. This guide focused experimental characterization efforts.

4. Simulation of the printing process:

- To account for the effects of printing, a coupled thermo-mechanical analysis can be performed to simulate the heat of hydration and subsequent thermal stresses that develop during the layer-by-layer deposition and curing process.

- Model the initial stress state induced by the weight of subsequent layers (buildability effects) as a pre-load before applying the compressive test load.

By systematically implementing these advanced modeling techniques, future simulations can transition from providing general observations to delivering high-fidelity predictions, thereby becoming a more reliable tool for the design and optimization of 3D printed concrete structures.

4 Conclusion

This study presented a comprehensive investigation into the compressive behavior of 3D-printed concrete (3DPC) through comparative analysis of experimental data and numerical simulations performed using ANSYS 2024. However, the comparison between experimental and simulated results revealed notable discrepancies ranging from minimal error levels (<3%) to substantial deviations (>60%) arising primarily from variations in mix composition, anisotropy, curing conditions, and simplifications in the numerical modeling process. The systematic review of selected studies demonstrated that accurate prediction of compressive strength in 3DPC depends on several critical parameters, such as inter-layer bonding quality, printing direction, and the presence of additives or fibers in the mix. In particular, the results emphasized that anisotropy and moisture conditions significantly influence the mechanical response, underscoring the necessity to refine numerical models to account for these factors explicitly.

Based on the analysis of the collected data, the mix in [25] with a w/c ratio of 0.4 and 30% GGBS replacement demonstrated an excellent balance of high compressive strength (60.2 MPa) and, as per the original study, satisfactory printability. For applications requiring lower early-age strength but potentially enhanced sustainability, geopolymer mixes like those in [21] and [24] show significant promise and warrant further optimization. As for laboratory settings, standard moist curing at >95% relative humidity and 23±2°C is recommended to ensure consistent and comparable results. For real-world construction, given the lack of formwork and large exposed surface area, a primary recommendation is the immediate application of curing compounds or membranes after printing to prevent plastic shrinkage and ensure continued hydration. The development of site-specific curing protocols that account for ambient temperature and humidity is crucial for achieving design strength in printed structures. Incorporating inter-layer interfaces, void distributions, and thermal mechanical coupling effects could substantially enhance the predictive accuracy of ANSYS models for 3DPC.

Overall, despite the current limitations, 3D printing of concrete remains a rapidly advancing technology with strong potential for large-scale structural applications. Continuous integration of experimental insights into computational models, along with further parametric and mesh sensitivity studies, will play a pivotal role in transforming 3D-printed concrete from a laboratory innovation into a reliable and standardized construction method.

Acknowledgments

The authors wish to acknowledge that there was no financial support or grant for this work.

References

[1] Sanjayan, J.G., Nazari, A., & Nematollahi, B. (2019). 3D concrete printing technology: Construction and building applications. Print.

[2] Perrot, A. (2019). 3D printing of concrete. UK: Print.

[3] Karslioglu, A., Alkayis, M.H., & Onur, M. (2022). 3D printing technology in construction sector: A short review. In International Conference on Applied Engineering and Natural Sciences, Turkey.

[4] Tay, Y.W.D., Panda, B., Paul, S.C., Mohamed, N.A.N., Tan, M.J., & Leong, K.F. (2017). 3D printing trends in building and construction industry: A review. *Virtual and Physical Prototyping*, 12(3), 261-276. https://doi.org/10.1080/17452759.2017.1326724.

[5] Khoshnevis, B. (2004). Automated construction by contour crafting—Related robotics and information technologies. *Automation in Construction*, 13(1), 5-19. https://doi.org/10.1016/j.autcon.2003.08.012.

[6] Hossain, M.A., Zhumabekova, A., Paul, S.C., & Kim, J.R. (2020). A review of 3D printing in construction and its impact on the labor market. *Sustainability*, 12(20), 8492. https://doi.org/10.3390/su12208492.

[7] Bazli, M., Ashrafi, H., Rajabipour, A., & Kutay, C. (2023). 3D printing for remote housing: Benefits and challenges. *Automation in Construction*, 148, Article 104772. http://dx.doi.org/10.1016/j.autcon.2023.104772.

[8] Filip, G.A., Abanda, F.H., & Fru, F.A. (2023). Construction 3D-printing in reducing the incidence of long latency respiratory diseases among construction workers in the UK. *Safety in Extreme Environments*, 5, 177-197. https://doi.org/10.1007/s42797-023-00078-4.

[9] El-Sayegh, S., Romdhane, L., & Manjikian, S. (2020). A critical review of 3D printing in construction: Benefits, challenges, and risks. *Archives of Civil and Mechanical Engineering*, 20, Article 34. https://doi.org/10.1007/s43452-020-00038-w.

[10] Suvash Chandra Paul, van Zijl, G.P.A.G., Tan, M.J., & Gibson, I. (2018). A review of 3D concrete printing systems and materials properties: Current status and future research prospects. *Rapid Prototyping Journal*. https://doi.org/10.1108/RPJ-09-2016-0154.

[11] Hameed, R., & Papon, A. (2019). Étude numérique du comportement d'un élément en béton imprimé en 3D. In *DiXite3dPrint: Fabrication additive pour la construction. Quelle actualité*

nationale? École des Ponts ParisTech, January 17-18, 2019, Champs-sur-Marne, France. HAL Id: hal-02119257. Retrieved from https://enpc.hal.science/hal-02119257.

[12] Feng, P., Meng, X., Chen, J.-F., & Ye, L. (2015). Mechanical properties of structures 3D printed with cementitious powders. *Construction and Building Materials*, *93*, 486–497. https://doi.org/10.1016/j.conbuildmat.2015.05.132.

[13] Shakor, P., Gowripalan, N., & Rasouli, H. (2021). Experimental and numerical analysis of 3D printed cement mortar specimens using inkjet 3DP. *Archives of Civil and Mechanical Engineering*, *21*, Article 58. https://doi.org/10.1007/s43452-021-00209-3.

[14] Aghajani Delavar, M., Chen, H., & Sideris, P. (2022). Design of 3D printed concrete walls under in-plane seismic loading. In *Proceedings of the 12th National Conference on Earthquake Engineering*, Earthquake Engineering Research Institute, Salt Lake City, UT.

[15] Li, F., Hu, X., & Shahzad, Q. (2025). Anisotropic behavior in 3D printed concrete: Finite element simulation approach. *Journal of Advanced Construction Materials*, *12*(3), 45-60.

[16] Xiao, J., Liu, H., & Ding, T. (2021). Finite element analysis on the anisotropic behavior of 3D printed concrete under compression and flexure. *Additive Manufacturing*, *39*, 101712. https://doi.org/10.1016/j.addma.2020.101712.

[17] Kaliyavaradhan, S. K., Ambily, P. S., Prem, P. R., & Ghodke, S. B. (2022). Test methods for 3D printable concrete. *Preprint submitted to Elsevier*, August 10, 2022.

[18] Özalp, F., & Yilmaz, H. D. (2020). Fresh and hardened properties of 3D high-strength printing concrete and its recent applications. *Iranian Journal of Science and Technology, Transactions of Civil Engineering*, *44*(Suppl 1), 319–330. https://doi.org/10.1007/s40996-020-00370-4.

[19] Benamara, A. (2022). *Impression 3D de matériaux dédiés à la construction: De la définition des encres, maîtrise de l'impression à la performance des produits imprimés* (Doctoral dissertation, Civil Engineering, CY Cergy Paris Université).

[20] Baz, B., Aouad, G., Khalil, N., & Remond, S. (2020). Inter-layer reinforcement of 3D printed concrete elements. *Asian Journal of Civil Engineering*, *22*(3), 341–349. https://doi.org/10.1007/s42107-020-00317-0.

[21] Panda, B., Mohamed, N. A. N., Paul, S. C., Singh, G. B., Tan, M. J., & Šavija, B. (2019). The effect of material fresh properties and process parameters on buildability and interlayer adhesion of 3D printed concrete. *Materials*, *12*(13), 2149. https://doi.org/10.3390/ma12132149.

[22] Meurer, M., & Classen, M. (2021). Mechanical properties of hardened 3D printed concretes and mortars Development of a consistent experimental characterization strategy. *Materials*, *14*(4), 752. https://doi.org/10.3390/ma14040752.

[23] Panda, B., Paul, S. C., & Tan, M. J. (2017). Anisotropic mechanical performance of 3D printed fiber reinforced sustainable construction material. *Materials Letters*, *209*, 146–149. https://doi.org/10.1016/j.matlet.2017.07.123.

[24] Sanjayan, J. G., Nematollahi, B., Xia, M., & Marchment, T. (2018). Effect of surface moisture on inter-layer strength of 3D printed concrete. *Construction and Building Materials*, *172*, 468–475.

[25] Wern, C. T. H., & Ali, N. (2024). Fresh properties and compressive strength of 3D printing concrete containing GGBS with varies in water-cement ratio. *Recent Trends in Civil Engineering and Built Environment*, *5*(1), 205–215. https://doi.org/10.30880/rtcebe.2024.05.01.021.